THE JOURNAL OF PHYSICAL CHEMISTRY B

Article

pubs.acs.org/JPCB

Real-Time Monitoring on the Adsorption Process of Salicylic Acid onto Chitosan Membrane Using Dielectric Spectroscopy: Macroscale Concentration Polarization and Dynamics

Yuhong Li,[†] Weidong Gao,[†] Kongshuang Zhao,*[,‡] Gang Yang,[†] Zhonghe Zhu,[†] and Rongjing Cui[†]

[†]Jiangsu Laboratory of Advanced Functional Materials, School of Chemistry and Material Engineering, Changshu Institute of Technology, Changshu, 215500, China

[‡]College of Chemistry, Beijing Normal University, Beijing, 100875, China

ABSTRACT: The adsorption process of salicylic acid (SA) onto chitosan membrane is monitored in real time by the dielectric relaxation spectroscopy (DRS) method. A unique dielectric relaxation, which is related to the macroscale concentration polarization layers (CPLs) in the SA solution caused by the adsorption, is observed. By modeling the measured systems composed of the membrane, the CPLs, and the SA solution, the dielectric spectra are analyzed systematically on the basis of the interfacial polarization theory. The parameters about the constituent phases, i.e., the dielectric constant ε_m and the conductivity κ_m of the chitosan membrane, the conductivity distribution (κ_1 to κ_2), and the thickness d_{CPL} of the CPL, are obtained. The time-dependent ε_m and κ_m give insight into the microstate of the chitosan membrane during the adsorption. Furthermore, the time evolution of the conductivity gradient of the CPL, $\Delta\kappa/d_{CPL}$, is combined to interpret the adsorption mechanism. It is suggested that the noninvasive dielectric monitoring may be applied to many adsorption and release processes.

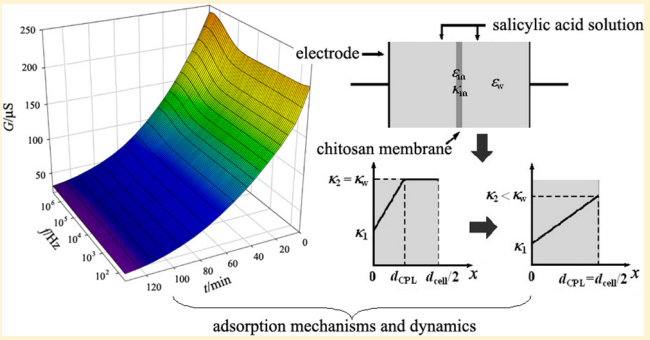

INTRODUCTION

Chitosan is an effective biosorbent that has gained wide attention because of its rich sources and high content of functional amino and hydroxyl groups.[1,2] It is of wide interest to monitor adsorption processes in situ and in real time to fully understand their dynamics, and thereby to explore the adsorption mechanisms (i.e., interactions between chitosan and the adsorbate). However, the question is how to choose the experimental method. A common method is to remove a certain volume of the solution from the adsorption system at set intervals and analyze the amount of the remaining adsorbate by appropriate spectrometric detections.[3−5] Obviously, this is an invasive and troublesome method. On the other hand, the interactions between the membrane and the adsorbates are usually statically examined by X-ray diffraction (XRD), infrared spectroscopy (IR), Fourier transform infrared spectroscopy (FT-IR), X-ray photoelectron spectroscopy (XPS), scanning electron microscopy (SEM), and atomic force microscopy (AFM),[6−8] independent of the study on the adsorption dynamics. These methods require the samples to be prepared specifically. Therefore, they are not suitable for continuously monitoring heterogeneous and dynamic adsorption processes. Dynamic properties of adsorption systems can be monitored by dielectric relaxation spectroscopy (DRS),[9−13] because it is noninvasive, easy to apply, and sensitive to heterogeneous systems.[14,15] On the basis of proper theoretical analysis, rich information on the adsorption dynamics and mechanisms will be obtained from the dielectric spectra.

In this study, the adsorption process of salicylic acid (SA) in aqueous solution onto chitosan membrane has been monitored by DRS experimentally and discussed theoretically. SA was chosen as a model organic pollutant because of its typical carboxyl, hydroxyl, and phenyl groups. In order to analyze the dielectric spectra and thereby to obtain the information on the adsorptive dynamics, a dielectric model is presented. This model considers (i) the interfacial polarization between the chitosan membrane and the bulk SA solution and (ii) the two concentration polarization layers (CPLs) developing at both sides of the chitosan membrane.

The studied system is a typical heterogeneous system composed of a polymer membrane and weak electrolyte solutions, and there are interfaces where phases of different dielectric constant ε and conductivity κ contact with each other. According to Maxwell−Wagner's interfacial polarization theory, dielectric relaxations due to interfacial polarization will be observed.[14,16−18] In detail, for a heterogeneous system with n phases that have distinct ε/κ values, theoretically, $n - 1$ Debye-type dielectric relaxations with different characteristic relaxation times will be observed. However, if the characteristic relaxation

Received: September 4, 2012
Revised: February 21, 2013

   dx.doi.org/10.1021/jp308758g | J. Phys. Chem. B XXXX, XXX, XXX−XXX

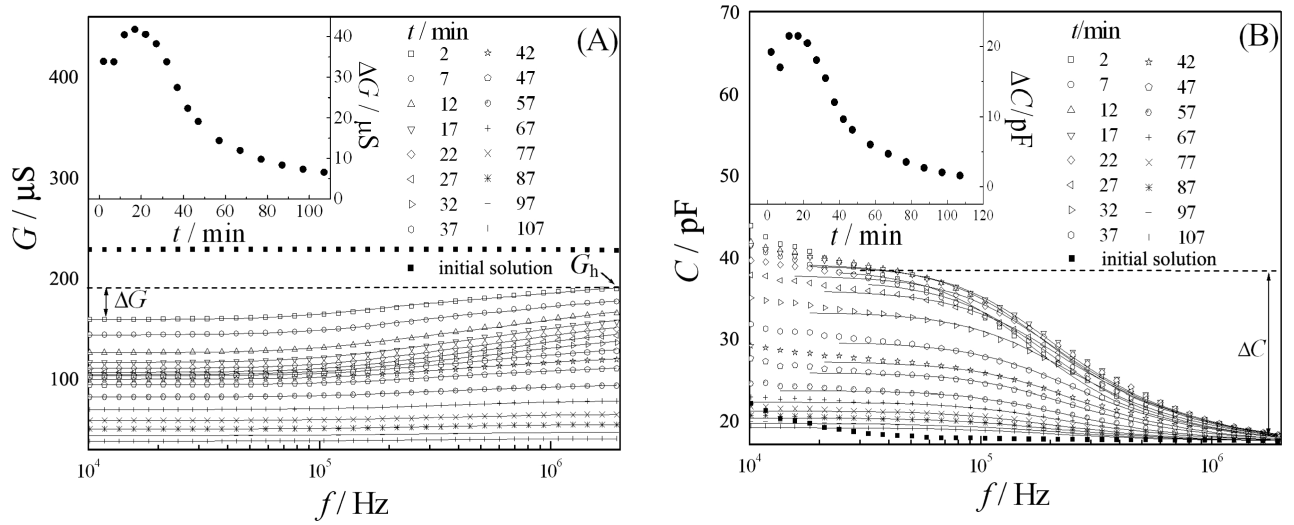

Figure 1. Frequency f dependence of conductance G (A) and capacitance C (B) for the system consisting of chitosan membrane and SA solution of 0.4 mmol/L, as a function of adsorption time t. Symbols denote experimental data, and solid lines are fitting curves according to eq 3. The dielectric response of the initial SA solution without the membrane is also shown.

times are close to each other, some of these relaxations will superimpose with each other and fewer dispersed Cole−Cole type relaxations will be observed.[14,15]

On the other hand, the concentration polarization concerned in our dielectric model contains several types in the literature. First, it is widely accepted as a micrometer-scale double layer polarization around the surface of particles suspended in electrolyte solution. It causes a dielectric relaxation in a low frequency range (usually between 10^{-7} and 10^{3} Hz, and very few around 10^{4} Hz).[19−22] Besides, Zhao et al.[23−26] have studied the dielectric relaxations caused by a macroscale (about 10^{-3} m thick) conductivity polarization layer near a charged membrane. This conductivity polarization is introduced by the applied dc bias voltage. The dielectric relaxation originates from the increase of impedance caused by the decline of one of the two boundary conductivities, and its characteristic frequency (between 10^{3} and 10^{6} Hz) depends upon the magnitude of the boundary conductivities. In addition, they have simulated another type of concentration polarization, a gradient in dielectric constant in the porous layer of a composite polymeric membrane. It also causes an obvious dielectric relaxation.[27] In the present study, the concentration polarization refers to a macroscale conductivity gradient, which is caused by the adsorption behavior of the chitosan membrane. The correlation between the dielectric relaxations and the CPL has been ascertained in a previous work from phenomenological discussions.[11]

The aim of the present study is to obtain the dynamic parameters about the CPL and to provide a method for monitoring the adsorption of charged solutes onto the membrane surface by analyzing time-dependent dielectric spectra. In addition, we also hope to provide insights into interpreting the adsorption mechanisms throughout the adsorption process by analyzing the time-dependent electrical parameters about the membrane.

1. EXPERIMENTAL SECTION

1.1. Materials. All of the chemicals used are of analytical grade unless otherwise stated. The chitosan powder, with a deacetylation degree of 88.63% and MW of 10^{6}, was purchased from Yuhuan Ocean Biochemistry Co. (Zhejiang, China). Salicylic acid (SA) was purchased from Beijing Chemical Reagent Co. (Beijing, China). NaOH and acetic acid were purchased from Beijing Beihua Fine Chemicals Co. (Beijing, China).

1.2. Preparation of Chitosan Membrane. Chitosan powder of 0.16 g was dissolved in 10 mL of 2% (v/v) acetic acid solution. The result solution was dropped on a piece of horizontal glass, and then left overnight under room temperature (20−21 °C) to evaporate the solvent. The chitosan membrane that formed on the leveled glass was then peeled off, immerged in 0.1 mol/L NaOH solution for 5 h, and rinsed with plenty of distilled water repeatedly, to remove the remaining acetic acid. Finally, a water-rich chitosan gel membrane was prepared, and its thickness is about 80 μm, which was measured with a vernier caliper. This membrane was verified to be water-permeable and homogeneous by measuring its dielectric spectrum in distilled water.[11]

1.3. Dielectric Measurements. Dielectric measurements were performed using an Agilent 4294A Precision Impedance Analyzer by applying an ac voltage of 100 mV amplitude, over a frequency (f) range from 40 Hz to 4 MHz, under 20−21 °C temperature. The studied cell system is described as follows: the chitosan membrane was sandwiched between a pair of cylindrical chambers, to whose ends two planar platinum electrodes were attached. Details of the measuring cell are described elsewhere.[28,29] After the measuring cell was quickly rinsed with some SA solution, the SA solution was injected into the chambers on both sides of the membrane. The frequency-dependent conductance (G) and capacitance (C) of the system, namely, the dielectric spectra, were immediately measured every 5 min, until the spectra did not change. The area (S) of each electrode, which is equal to that of the membrane, is 3.14 cm^2, and the cell constant (d_{cell}/S) is 0.414 cm^{-1} (d_{cell} is the distance between the two electrodes). The initial concentrations c_0 of SA are 0.1, 0.2, 0.4, and 0.6 mmol/L, respectively. The dielectric responses of the initial SA solutions (0.1, 0.2, 0.4, and 0.6 mmol/L) without the membrane were also measured to obtain the conductivity (κ_w) of these solutions.

dx.doi.org/10.1021/jp308758g | J. Phys. Chem. B XXXX, XXX, XXX−XXX

2. RESULTS AND DISCUSSION

2.1. Dielectric Spectra of the SA Adsorption Process by Chitosan Membrane. Figure 1 shows the dielectric spectra of the system composed of chitosan membrane and 0.4 mmol/L SA solution, measured as a function of adsorption time t. It is obvious from Figure 1 that a remarkable dielectric relaxation can be observed around 10^5 Hz. A dielectric relaxation refers to the increase of G and the simultaneous decrease of C around a same characteristic frequency f_0 (see Figure 2) as the frequency f increases. The intensity of a

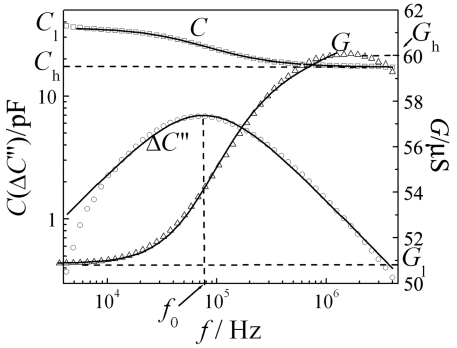

Figure 2. Fitting with the Cole−Cole equation on the dielectric spectrum of the adsorption of 0.1 mmol/L SA at 2 min. Symbols denote the experimental data, and curves denote the fitting result.

relaxation ΔG (or ΔC) is defined as the difference between the two limited conductance (or capacitance) values corresponding to two plateaus of a G−f curve (or a C−f curve), as depicted in Figure 1. From the insets of Figure 1, it is clear that, when the adsorption passes about 20 min, both of the relaxation intensities, ΔG and ΔC, show a maximum value. This will be discussed in section 2.2. Furthermore, the conductance at the high-frequency limit (G_h, Figure 1A) decreases over time, reflecting the adsorption of SA onto the membrane. This is because G_h is positively related with the concentration of free conductive materials (i.e., SA for this system) in the solution.[15,29] Another interesting phenomenon is that, when the adsorption approaches equilibrium after 100 min (the C−f and G−f curves almost do not vary over time), the dielectric relaxation tends to disappear (ΔG and ΔC tend to be zero). Dielectric spectra of the adsorption systems with other initial SA concentrations show a similar changing tendency with Figure 1.

2.2. Mechanism of the Dielectric Relaxations. To examine the characteristics of the dielectric spectra and to explore the origin of the relaxation, the following Cole−Cole equations[14] were employed to fit the experimental data (C and G, where the conductance G is converted to imaginary capacitance $\Delta C''$). Figure 2 shows a representative fitting result.

$$C = C_h + \frac{(C_l - C_h)[1 + (f/f_0)^{1-\alpha}\cos\{\pi(1-\alpha)/2\}]}{1 + 2(f/f_0)^{1-\alpha}\cos\{\pi(1-\alpha)/2\} + (f/f_0)^{2(1-\alpha)}} \quad (1a)$$

$$\Delta C'' = \frac{(C_l - C_h)(f/f_0)^{1-\alpha}\sin\{\pi(1-\alpha)/2\}}{1 + 2(f/f_0)^{1-\alpha}\cos\{\pi(1-\alpha)/2\} + (f/f_0)^{2(1-\alpha)}} \quad (1b)$$

where $\Delta C'' = (G - G_l)/(2\pi f)$ and C_l and C_h are the limit values of capacitances at low (subscript l) and high (h) frequencies, respectively. G_l is the limit conductance at low frequencies. f_0 is the characteristic relaxation frequency (see Figure 2), and α ($0 \leq \alpha < 1$) is the distribution parameter of the relaxation time τ ($\tau = (2\pi f_0)^{-1}$). The mean value of α obtained from the fitting is 0.18 for all membrane/SA solution systems. This means that the relaxations are not Debye type. For a Debye-type relaxation, $\alpha = 0$, which corresponds to a simple relaxation mechanism such as there is only one kind of interface or two homogeneous phases.[14] Therefore, the dispersed relaxation shown in Figure 1 originates from multiple mechanisms. In other words, maybe in addition to the conventional interfacial polarization between the chitosan membrane and the bulk SA solution, there are other unknown polarization mechanisms that also contribute to the dispersed relaxation.

In order to reveal these polarization mechanisms, an independent dielectric measurement was carried out by replacing the SA with sodium salicylate (SS) of the same concentration in the membrane/solution systems. Different from the membrane/SA system, no obvious dielectric relaxation is observed for the membrane/SS system and the dielectric spectra do not change over time, as shown in Figure 3. This shows that no adsorption process could be observed. In other words, in this work, SS in solution has barely been adsorbed onto the chitosan membrane. This may be explained as follows:

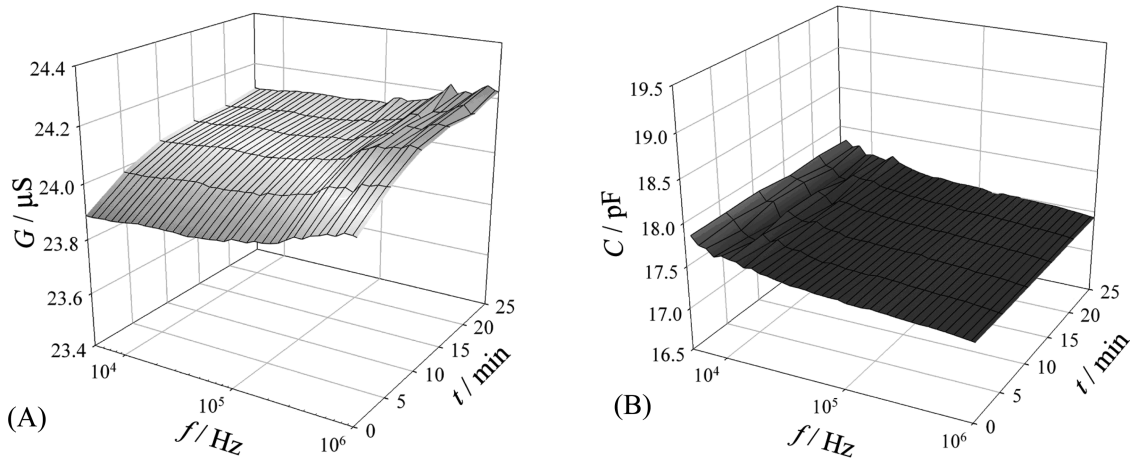

Figure 3. Dielectric response of the chitosan membrane−0.1 mmol/L SS system. Conductance G (A) and capacitance C (B) against time t and frequency f. The slight increase of conductance G over time may be due to the dissolving of CO_2 from air.

dx.doi.org/10.1021/jp308758g | J. Phys. Chem. B XXXX, XXX, XXX−XXX

SS solution and SA solution have alkaline and acidic pH, respectively; the $-NH_2$ residues of the chitosan membrane are less protonated in the SS solution than in the SA solution, resulting in no adsorption in the membrane/SS system.

Now we return to the main question about the relaxation mechanism of the membrane/SA system. Comparing the measuring results for the membrane/SA and membrane/SS systems, two conclusions can be drawn. First, the relaxation of the membrane/SA system is not caused only by the interfacial polarization between the membrane and the solution. If so, a relaxation should also be observed for the membrane/SS system, because there is no essential difference between SA and SS aqueous solutions in ε or κ. Therefore, there must be another unevenly distributed property that leads to the dielectric relaxation of the membrane/SA system. Second, the dielectric relaxation is accompanied by the adsorption behavior. This can be easily interpreted by introducing the CPL. The adsorption of SA onto the chitosan membrane causes the decrease of the concentration of free SA near the membrane and the directional migration of SA in the solution. This results in CPLs alongside the membrane, and the CPLs then cause remarkable dielectric relaxation. In short, the CPLs connect the adsorption behavior with the dielectric relaxation. This conjecture is supported by the experimental results shown in the insets of Figure 1 where the relaxation intensities (ΔG and ΔC) show an inflection point during the adsorption process. The relaxation intensities caused by CPL are dominated by two factors, one of which is the conductivity distribution and the other is the thickness of the CPL, as reported in our previous work.[11] The complex changes of these two factors during the adsorption processes lead to the nonmonotonic change of ΔG and ΔC.

On the other hand, the electrical parameters of the chitosan membrane (ε_m and κ_m) will certainly be changed by the adsorption, which is a secondary factor that causes the dielectric relaxation.

On the basis of the above discussions, the dielectric relaxation of the membrane/SA system can be discussed by considering both the influence of the CPLs developing alongside the membrane and the interfacial polarization between the chitosan membrane and the SA solution.

2.3. Electrical Model and Analyzing Method. In order to ascertain the relaxation mechanisms, and to examine the adsorption dynamics, it is necessary to estimate the electric and architectural properties of each constituent of the membrane/SA solution system. For this purpose, an electrical model shown in Figure 4 is established from a dielectric perspective. Figure 4A shows the schematic diagram for the whole system in which the chitosan membrane with homogeneous dielectric constant ε_m and conductivity κ_m is sandwiched between two SA solutions with a dielectric constant of ε_w. Two CPLs exist in the solutions symmetrically, adjoining the membrane. The conductivities of both CPLs are κ_1 on the membrane side and linearly increase to κ_2 on the bulk solution side. With the processing of the adsorption, the values of κ_2 and κ_w (conductivity of the initial SA solution) meet the following relationships in turn during the initial part and the later part of the adsorption process, respectively:

$$\kappa_2 \begin{cases} = \kappa_w & (d_{CPL} < d_{cell}/2) \\ \leq \kappa_w & (d_{CPL} = d_{cell}/2) \end{cases} \tag{2}$$

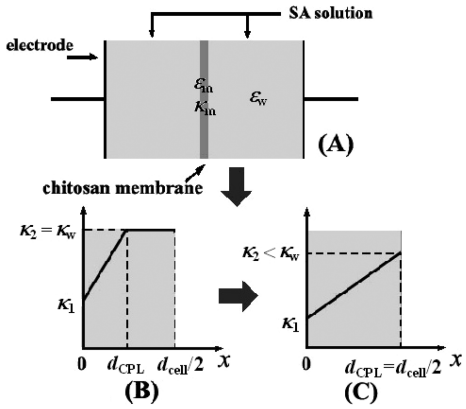

Figure 4. Schematic diagram of the measured membrane/SA system (A) and electrical model of the CPL (B and C, corresponding to initial and later periods of the adsorption process, respectively). 0 denotes the location x at the membrane surface.

where d_{CPL} is the thickness of the CPL and d_{cell} is the distance between the two electrodes as mentioned above; the equality and inequality correspond to Figure 4B and C, respectively.

The total reciprocal complex capacitance of the layered system C^*_{sys} depicted in Figure 4A can be expressed by

$$\frac{1}{C^*_{sys}} = \frac{2}{C^*_p(f)} + \frac{1}{C^*_m} + \frac{1}{C^*_w} \tag{3}$$

where $C^*_p(f)$, C^*_m, and C^*_w are the complex capacitance of the CPL, the chitosan membrane, and the bulk SA solution, respectively. The complex capacitance C^* of the whole system and of each component is defined as

$$C^* = C - jC'' = C + \frac{G}{j2\pi f} \tag{4}$$

where C and C'' are the real and imaginary parts of C^*, respectively. $C'' = G/(2\pi f)$, obviously.

The conductance and capacitance of the bulk solution (subscript w) and the chitosan membrane (m) in eqs 3 and 4 (G_w, G_m, C_w, C_m) are substituted by functions of corresponding conductivity and dielectric constant (κ_w, κ_m, ε_w, ε_m):

$$G = \frac{\kappa S}{d} \tag{5a}$$

$$C = \frac{\varepsilon \varepsilon_0 S}{d} \tag{5b}$$

where $\varepsilon_0 = 8.8542 \times 10^{-12}$ F·m^{-1} is the vacuum dielectric constant and d is the thickness of the corresponding layer.

On the other hand, the conductance and capacitance of the CPL ($G_p(f)$ and $C_p(f)$) can be expressed by[25]

$$G_p(f) = \frac{S(\kappa_2 - \kappa_1)}{d_{CPL}} \frac{A}{A^2 + B^2} \tag{6a}$$

$$C_p(f) = \frac{S(\kappa_2 - \kappa_1)}{d_{CPL}} \frac{\frac{B}{\omega}}{A^2 + B^2} \tag{6b}$$

where $\omega = 2\pi f$ is the angular frequency of the applied ac electric field. A and B are functions of κ_1 and κ_2, as expressed by

dx.doi.org/10.1021/jp308758g | J. Phys. Chem. B XXXX, XXX, XXX–XXX

Table 1. Parameters Obtained from Fitting with eq 3 for the Case of Chitosan Membrane Adsorbing 0.4 mmol/L SA

t (min)	ε_w	ε_m	κ_m (μS·cm^{-1})	κ_1 (μS·cm^{-1})	κ_2 (μS·cm^{-1}	d_{CPL} (mm)	R^2
2	82.0 ± 0.3	37.0 ± 1.7	3.00 ± 0.10	30.7 ± 1.2	94.6	2.4 ± 0.1	0.9999895
7	82.0 ± 0.2	24.0 ± 1.6	2.20 ± 0.10	31.2 ± 1.2	94.6	3.2 ± 0.1	0.9999919
12	81.5 ± 0.3	20.2 ± 1.7	1.71 ± 0.09	22.9 ± 1.0	94.6	3.5 ± 0.1	0.9999954
17	82.5 ± 0.3	16.1 ± 1.4	1.40 ± 0.07	21.8 ± 0.9	94.6	3.9 ± 0.1	0.9999959
22	82.5 ± 0.4	14.4 ± 1.3	1.28 ± 0.07	21.6 ± 0.8	94.6	4.4 ± 0.1	0.9999959
27	83.9 ± 0.4	12.9 ± 1.1	1.21 ± 0.09	22.8 ± 0.8	94.6	4.9 ± 0.1	0.9999964
32	83.9 ± 0.4	12.1 ± 1.3	1.21 ± 0.08	24.8 ± 0.9	94.6	5.7 ± 0.1	0.9999961
37	84.0 ± 0.3	12.4 ± 1.2	1.35 ± 0.10	27.1 ± 0.8	92.0 ± 3.3	6.5	0.9999940
42	84.0 ± 0.3	13.1 ± 1.1	1.47 ± 0.09	28.0 ± 0.8	81.3 ± 3.5	6.5	0.9999947
47	84.5 ± 0.2	13.4 ± 1.2	1.49 ± 0.08	28.0 ± 0.9	72.0 ± 3.0	6.5	0.9999970
57	84.5 ± 0.4	14.0 ± 1.3	1.50 ± 0.08	25.6 ± 0.7	57.9 ± 3.2	6.5	0.9999982
67	84.5 ± 0.3	15.0 ± 1.3	1.50 ± 0.07	21.1 ± 0.6	48.5 ± 2.8	6.5	0.9999987
77	84.2 ± 0.4	16.0 ± 1.3	1.46 ± 0.08	18.0 ± 0.6	39.4 ± 2.6	6.5	0.9999980
87	84.2 ± 0.3	17.0 ± 1.2	1.46 ± 0.06	15.4 ± 0.5	32.8 ± 2.3	6.5	0.9999978
97	84.2 ± 0.3	17.5 ± 1.3	1.46 ± 0.07	13.7 ± 0.4	27.7 ± 2.5	6.5	0.9999993
107	84.2 ± 0.2	17.9 ± 1.4	1.46 ± 0.08	12.1 ± 0.5	23.6 ± 2.4	6.5	0.9999993
127	83.9 ± 0.1	18.4 ± 1.3	1.46 ± 0.08	10.4 ± 0.4	18.4 ± 2.0	6.5	0.9999996
137	83.9 ± 0.4	18.3 ± 1.3	1.47 ± 0.07	10.4 ± 0.5	16.1 ± 1.7	6.5	0.9999996
147	83.7 ± 0.3	18.5 ± 1.4	1.47 ± 0.07	9.9 ± 0.5	14.6 ± 1.3	6.5	0.9999974

$$A = \frac{1}{2}\ln\left(1 + \frac{\left(\frac{\kappa_2}{\kappa_1}\right)^2 - 1}{1 + \left(\frac{\varepsilon_w\varepsilon_0}{\kappa_1}\right)^2\omega^2}\right) \quad (7)$$

$$B = \tan^{-1}\frac{(\kappa_2 - \kappa_1)\omega\varepsilon_w\varepsilon_0}{(\omega\varepsilon_w\varepsilon_0)^2 + \kappa_2\kappa_1} \quad (8)$$

where ε_w is the relative dielectric constant of the CPL, equal to that of the bulk SA solution.

The curve-fitting is carried out on the real part C and imaginary part C'' of the complex capacitance C^*_{sys} as a function of frequency f in eq 3 by the least-squares method to minimize the sum of the squares of the errors, χ^2:

$$\chi^2 = \sum_{i=1}^{N}\{[C_e(f_i) - C_t(f_i)]^2 + [C''_e(f_i) - C''_t(f_i)]^2\} \quad (9)$$

where N denotes the number of applied frequencies and the subscripts e and t refer to the experimental and theoretical values, respectively. The fitting gives the values of ε_w, ε_m, κ_m, κ_1, κ_2, and d_{CPL}. κ_w is a fixed value in the fitting procedure, which is obtained by measuring the initial SA solution. These parameters for the system with 0.4 mmol/L initial SA concentration are shown in Table 1, where the correlation coefficients of all fittings are higher than 0.99998. The comparison of the fitting curves to the experimental data is shown in Figure 1. It can be seen that the fitting curves agree with the experimental data well, except for some discrepancy with the C–f data for the first 20 min of the adsorption. This discrepancy may be attributed to the initial fast adsorption that makes the property of the membrane surface a little different from that inside the membrane.

2.4. Dielectric Constant and Conductivity of Membrane and the Adsorption Mechanism. For clarity, the parameters ε_w and ε_m in Table 1 are plotted as a function of adsorption time t in Figure 5A. As can be seen, the dielectric constant of the solution, ε_w, is independent of the adsorption time and close to that of water at room temperature, 80. It is reasonable. While the dielectric constant of the membrane, ε_m,

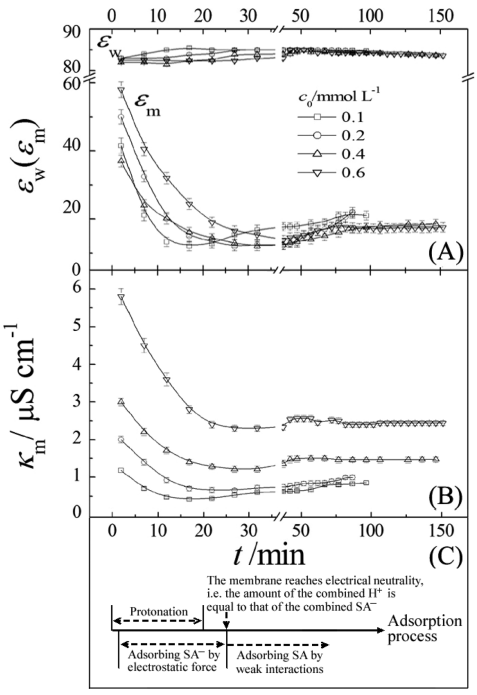

Figure 5. Dielectric constant of the solution (ε_w) and of the chitosan membrane (ε_m) (A) and conductivity of the membrane (κ_m) (B) vs time t, obtained from fitting with eq 3. Schematic diagram of the behavior or state of the membrane during the adsorption process (C).

sharply decreases to the minimum within the first 15–35 min (varying with SA concentrations c_0), it then increases slightly until it reaches a steady value. The change of ε_m as the function of adsorption time t can be interpreted from three aspects as follows.

First, the contribution of water in pores of the membrane should be taken into account. The high dielectric constant of water (around 80) pulls up the values of ε_m on the whole, resulting in the dielectric constant of the whole membrane ε_m (12–58) being much higher than that of chitosan powder (for most polymers usually 2–10).

dx.doi.org/10.1021/jp308758g | J. Phys. Chem. B XXXX, XXX, XXX–XXX

Second, the double layers of the pores in the membrane also contribute to ε_m. In detail, some of the H^+ ions from ionization of SA are immediately adsorbed onto the $-NH_2$ groups of chitosan molecules to form $-NH_3^+$ due to the protonation effect of $-NH_2$. This initial process was not observed because it is too fast. Therefore, the membrane becomes positively charged, and the double layers appear alongside the membrane pores. The effective capacitance of the membrane C_m contributed by the double-layer capacitances C_{di} is derived according to the dielectric model proposed by Nakamura,[30] where C_m is considered as the geometric mean of a series combination and a parallel combination of the capacitances of each double layer. It is expressed as

$$C_m = \frac{\varepsilon_m \varepsilon_0 S}{d_m} = \sqrt{\left(\sum_{i=1}^{N'} \frac{1}{C_{di}}\right)^{-1} \sum_{i=1}^{N'} C_{di}} \quad (10)$$

where d_m is the thickness of the membrane and N' is the number of double layers that are randomly distributed in the membrane. It is obvious from eq 10 that ε_m is positively related to any double-layer capacitance C_{di}. Furthermore, according to the classical Gouy−Chapman double-layer model,[31−33] a higher fixed charge content c_f on the wall of the membrane pores corresponds to a higher double-layer capacitance C_{di}. Therefore, the sharp decrease of ε_m within the first tens of minutes of the adsorption process (see Figure 5A) may be due to the decrease in c_f. This shows the membrane rapidly adsorbs more salicylate anions (denoted as SA^- hereafter) than H^+ in this stage due to the electrical potential difference between the membrane and the bulk solution. As a result, the positive fixed charges of the membrane are reduced.

Finally, after ε_m decreases to the minimum, it increases slightly until it reaches a steady value (Figure 5A). This implies that the membrane reaches electrical neutrality (i.e., the positive fixed charges on the chitosan molecules, $-NH_3^+$, are balanced by the combined SA^-) and then mainly adsorbs electrically neutral SA molecules depending on some weak interactions, such as van der Waals forces, hydrophobic force, etc. The weak interactions have been verified due to the fact that a part of the adsorbed SA molecules can be released into distilled water.[11] The slow increase of ε_m in this stage is ascribed to the combination of SA molecules, because SA is a compound of strong polarity.

Figure 5B shows the plots of the membrane conductivity, κ_m, against the adsorption time t for various initial SA concentrations c_0. It is obvious that the changing trend of κ_m over time is similar to that of Figure 5A. The difference is that κ_m is positively dependent on c_0, suggesting the permeation of the solution into the membrane phase. The values of κ_m for different initial concentrations c_0 drop to the minimum within the first 15−35 min. This may be ascribed to the following reason: the combination of SA^- by $-NH_3^+$ on the chitosan chains results in the decrease of the positive fixed charge content (c_f) on the membrane; as a result, the concentration of the ions in the double layers in the membrane pores decreases.

The slow increase of κ_m after dropping to a minimum is because of the adsorption of neutral SA molecules in this stage, as discussed in the explanation for ε_m. In detail, the combination of SA by weak interactions will reach an adsorption−desorption equilibrium: the more the SA combined with the chitosan molecules, the more the SA that dissolves in the solution within the membrane pores.

On the basis of above interpretations about the time dependence of ε_m and κ_m, we suggest an adsorption mechanism and depict it in Figure 5C. In detail, the H^+ from ionization of SA are adsorbed by $-NH_2$ groups on the chitosan membrane through a protonation effect, and SA^- is adsorbed due to the electric potential difference between the membrane and the solution. These two effects exist simultaneously except for a little advance of the protonation of $-NH_2$. After the membrane reaches electrical neutrality, the membrane adsorbs SA molecules by some weak interactions.

2.5. Characteristics of the CPL. Figure 6 shows the time-dependent structural and electrical properties of the CPL (the thickness d_{CPL} and the conductivities of both sides of the CPL, κ_1 and κ_2) during the adsorption processes. First, we compare Figure 6A and C. It is clear that d_{CPL} increases monotonously within about the first 30 min until it reaches the maximum value $d_{cell}/2$ and then keeps unchanged. This means that the CPL becomes thicker until it expands to the entire solution with the proceeding of the adsorption. Correspondingly, in about the first 30 min, the values of κ_2 keep invariable (equal to κ_w), and then decrease gradually. This is because the influence of the adsorption on κ_2 is buffered by the expansion of the thickness of the CPL.

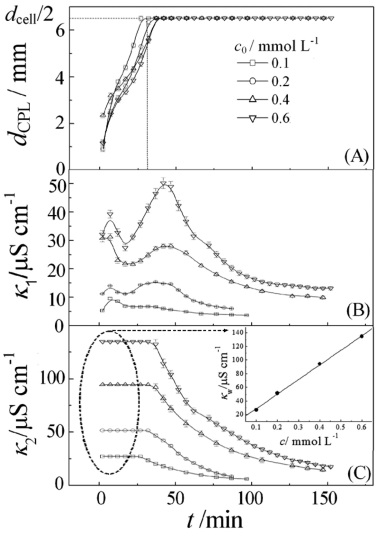

Figure 6. The time dependence of the thickness d_{CPL} (A), the conductivity at the side adjoining the membrane κ_1 (B), and that at the side adjoining the bulk solution κ_2 (C) of the CPL, in SA solutions of various concentrations.

Now we turn to Figure 6B to discuss the conductivity κ_1 of the CPL on the side adjoining the membrane. It is clear that κ_1 fluctuates sharply in the first 40 min and then decreases gradually. This is because κ_1 is influenced by two factors. One is the adsorption of the membrane, which decreases κ_1; the other is the migration of the SA molecules in CPLs from bulk solution toward the membrane, which increases κ_1. In the initial period of the adsorption process, the adsorption rate is very quick and decreases fast, as can be seen in Figure 7. Therefore, the CPLs are unstable, which results in the sharp fluctuation of κ_1. In the later period of the adsorption process, the adsorption rate slows down and the structure of the CPLs becomes stable. As a result, κ_1 gradually decreases.

2.6. Adsorption Rate and Dynamics. By using the structural and electrical parameters of the CPL, the parameters

dx.doi.org/10.1021/jp308758g | J. Phys. Chem. B XXXX, XXX, XXX−XXX

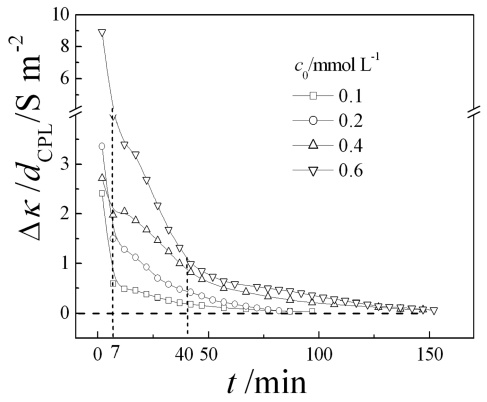

Figure 7. Conductivity gradient of the CPL $\Delta\kappa/d_{CPL}$ in the adsorption processes against time t. $\Delta\kappa/d_{CPL}$ is in proportion to the adsorption rate.

correlated to the adsorption rate can be estimated according to Fick's diffusion law:

$$\frac{dm}{dt} = DS\frac{dc}{dx} \tag{11}$$

where dm/dt is the diffusion amount through a cross section (with an area of S) of the CPL in unit time; dc/dx is the concentration gradient; D is the diffusion coefficient. In this study, because the intrinsic reason of the diffusion of SA across the CPL is the adsorption effect of the membrane, the diffusion rate dm/dt can be considered as the adsorption rate approximately. In addition, since the concentration c of the SA solution in this study is proportional to the conductivity κ (see the inset in Figure 6C), the following relationship will be observed:

$$\frac{dm}{dt} \propto \frac{\Delta\kappa}{d_{CPL}} \tag{12}$$

where $\Delta\kappa = \kappa_2 - \kappa_1$. This equation shows that the change of the conductivity gradient $\Delta\kappa/d_{CPL}$ over time reflects the characteristics of the adsorption behavior.

Figure 7 shows the time dependence of the conductivity gradient, $\Delta\kappa/d_{CPL}$, for different SA concentrations c_0. As can be seen, $\Delta\kappa/d_{CPL}$ decreases at a different rate in three stages separated by two flex points at about 7 and 40 min, respectively. In the first 7 min, the adsorption rate is the fastest. This is due to the intense protonation of the $-NH_2$ groups on the surface of the chitosan membrane and the simultaneous fast combination of SA^- due to the large potential difference between the membrane and the solution caused by the fixed charges ($-NH_3^+$). In about 7–40 min, the adsorption rate is still fast but noticeably slower compared with the first 7 min. This is because in this stage the adsorption is dominated by the protonation of $-NH_2$ groups and subsequent adsorption on SA^- inside the membrane, so the adsorption rate is restrained by the diffusion of the solute in the membrane. In addition, the decrease in the amount of the $-NH_2$ residues due to the continuous adsorption also account for the decrease of the adsorption rate. After 40 min, the adsorption rate becomes still smaller and gradually tends to 0, suggesting that the adsorption reaches equilibrium. The low adsorption rate is ascribed to the weak interactions between chitosan and SA that dominate in this stage.

3. CONCLUSIONS

Dielectric spectroscopy is used to monitor the adsorption process of salicylic acid (SA) onto chitosan membrane. To analyze the dielectric spectra theoretically, a multilayer electric model is proposed by modeling the studied system composed of chitosan membrane, CPLs, and bulk solution. On the basis of this model, the time-dependent dielectric constant and conductivity of the chitosan membrane (ε_m and κ_m), thickness, and conductivity distribution profile of the CPL (d_{CPL}, κ_1 to κ_2) are obtained.

By analyzing the time-dependent ε_m and κ_m, the adsorption mechanisms are estimated: the protonation of $-NH_2$ groups on the chitosan molecules gives rise to an electric potential difference between the membrane and the solution; the SA^- are simultaneously combined by the membrane due to this electric potential difference; after the membrane reaches electrical neutrality, SA molecules are adsorbed by some weak interactions. Furthermore, the time-dependent conductivity gradient of the CPL, $\Delta\kappa/d_{CPL}$, indicates that the adsorption processes can be divided into three stages at different adsorption rates. The adsorption mechanism of each stage is interpreted.

It is worth mentioning that the formation of CPL is the key to monitoring the adsorption process. The dielectric spectroscopy method can sensitively detect the presence and change of CPL, regardless of the molecular structure of the concerned charged solutes (if only a CPL forms). The dielectric analysis can give the structural and electrical properties of the CPL, which contributes a lot in discussing the adsorption dynamics and mechanisms. Since CPL associates with most mass transfer processes in liquid systems, such as adsorption and enrichment of heavy metal ions by water treatment reagent, sustained release of drug or fertilizer from carriers, etc., this study suggests that dielectric spectroscopy is very promising to be applied to most adsorption or release systems, both for real-time monitoring and for exploring the dynamics.

AUTHOR INFORMATION

Corresponding Author

*E-mail: zhaoks@bnu.edu.cn. Phone: +8601058808283. Fax: +8601058808283.

Notes

The authors declare no competing financial interest.

ACKNOWLEDGMENTS

The financial support of the National Natural Science Foundation of China (20976015, 20905010, 21173025) and of the NSF of Jiangsu Educational Department of China (10KJA480001) is gratefully acknowledged.

REFERENCES

(1) Hasan, S.; Krishnaiah, A.; Ghosh, T. K.; Viswanath, D. S. Adsorption of Divalent Cadmium (Cd(II)) from Aqueous Solutions onto Chitosan-Coated Perlite Beads. *Ind. Eng. Chem. Res.* **2006**, *45*, 5066–5077.

(2) Crini, G.; Badot, P.-M. Application of Chitosan, a Natural Aminopolysaccharide, for Dye Removal from Aqueous Solutions by Adsorption Processes Using Batch Studies: A Review of Recent Literature. *Prog. Polym. Sci.* **2008**, *33*, 399–447.

(3) Grisdanurak, N.; Akewaranugulsiri, S.; Futalan, C. M.; Tsai, W. C.; Kan, C. C.; Hsu, C. W.; Wan, M. W. The Study of Copper Adsorption from Aqueous Solution Using Crosslinked Chitosan Immobilized on Bentonite. *J. Appl. Polym. Sci.* **2012**, *125*, E132–E142.

dx.doi.org/10.1021/jp308758g | *J. Phys. Chem. B* XXXX, XXX, XXX–XXX

(4) Debrassi, A.; Baccarin, T.; Demarchi, C. A.; Nedelko, N.; Ślawska- Waniewska, A.; Dłużewski, P.; Bilska, M.; Rodrigues, C. A. Adsorption of Remazol Red 198 onto Magnetic N-Lauryl Chitosan Particles: Equilibrium, Kinetics, Reuse and Factorial Design. *Environ. Sci. Pollut. Res.* **2012**, *19*, 1594−1604.
(5) Zhang, J.; Chen, X. G.; Huang, L.; Han, J. T.; Zhang, X. F. Self-Assembled Polymeric Nanoparticles Based on Oleic Acid-Grafted Chitosan Oligosaccharide: Biocompatibility, Protein Adsorption and Cellular Uptake. *J. Mater. Sci.: Mater. Med.* **2012**, *23*, 1775−1783.
(6) Jin, L.; Bai, R. B. Mechanisms of Lead Adsorption on Chitosan/PVA Hydrogel Beads. *Langmuir* **2002**, *18*, 9765−9770.
(7) Indest, T.; Laine, J.; Ribitsch, V.; Johansson, L.-S.; Stana-Kleinschek, K.; Strnad, S. Adsorption of Chitosan on PET Films Monitored by Quartz Crystal Microbalance. *Biomacromolecules* **2008**, *9*, 2207−2214.
(8) Chang, X. H.; Chen, D. R.; Jiao, X. L. Chitosan-Based Aerogels with High Adsorption Performance. *J. Phys. Chem. B* **2008**, *112*, 7721−7725.
(9) Bonincontro, A.; Falivene, M.; La Mesa, C.; Risuleo, G.; Peña, M. R. Dynamics of DNA Adsorption on and Release from SDS−DDAB Cat−Anionic Vesicles: a Multitechnique Study. *Langmuir* **2008**, *24*, 1973−1978.
(10) Nicolas, A.; Devautour-Vinot, S.; Maurin, G.; Giuntini, J. C.; Henn, F. Cation Dynamics upon Adsorption of Methanol in Na−Y Faujasite Type Zeolites: A Dielectric Relaxation Spectroscopy Investigation. *J. Phys. Chem. C* **2007**, *111*, 4722−4726.
(11) Li, Y. H.; Zhao, K. S.; Han, Y. Dielectric Study on Membrane Adsorption and Release: Relaxation Mechanism and Diffusion Dynamics. *Sci. China, Ser. B: Chem.* **2008**, *51*, 813−822.
(12) Chen, Z.; Ni, N.; Zhao, K. S. Real-Time Monitor on the Release of Salicylic Acid from Chitosan Gel Beads by Means of Dielectric Spectroscopy. *Colloid Polym. Sci.* **2010**, *288*, 1245−1253.
(13) Lu, Q.; Zhao, K. S. Dielectric Spectroscopy of a Nanofiltration Membrane -Electrolyte Solution System: I. Low-Frequency Dielectric Relaxation from the Counterion Polarization in Pores and Model Development. *J. Phys. Chem. B* **2010**, *114*, 16783−16791.
(14) Asami, K. Characterization of Heterogeneous Systems by Dielectric Spectroscopy. *Prog. Polym. Sci.* **2002**, *27*, 1617−1659.
(15) Zhao, K. S.; Li, Y. H. Dielectric Characterization of a Nanofiltration Membrane in Electrolyte Solutions: Its Double-Layer Structure and Ion Permeation. *J. Phys. Chem. B* **2006**, *110*, 2755−2763.
(16) Maxwell, J. C. *Treatise on Electricity and Magnetism*; Clarendon Press: Oxford, U.K., 1891.
(17) Wagner, K. W. Erklärung der Dielektrishen Nachwirkungsvorgänge auf Grund Maxerllsher Vorstellungen. *Arch. Elektrotech. (Berlin)* **1914**, *2*, 371−387.
(18) Hanai, T.; Zhang, H. Z.; Sekine, K.; Asaka, K.; Asami, K. The Number of Interfaces and the Associated Dielectric Relaxations in Heterogeneous Systems. *Ferroelectrics* **1988**, *86*, 191.
(19) Schwarz, G. A Theory of the Low-Frequency Dielectric Dispersion of Colloidal Particles in Electrolyte Solution. *J. Phys. Chem.* **1962**, *66*, 2636−2642.
(20) Chew, W. C.; Sen, P. N. Dielectric Enhancement due to Electrochemical Double Layer: Thin Double Layer Approximation. *J. Phys. Chem.* **1982**, *77*, 4683−4693.
(21) Grosse, C. Permittivity of a Suspension of Charged Spherical Particles in Electrolyte Solution. 2. Influence of the Surface Conductivity and Asymmetry of the Electrolyte on the Low- and High-Frequency Relaxations. *J. Phys. Chem.* **1988**, *92*, 3905−3910.
(22) Shilov, V. N.; Delgado, A. V.; Gonzalez-Caballero, F.; Grosse, C. Thin Double Layer Theory of the Wide-Frequency Range Dielectric Dispersion of Suspensions of Non-conducting Spherical Particles Including Surface Conductivity of the Stagnant Layer. *Colloids Surf., A* **2001**, *192*, 253−265.
(23) Zhao, K. S.; Yasuhiro, M.; Asaka, K.; Asami, K.; Hanai, T. Dielectric Analysis of Concentration Polarization Phenomena at Cationexchange Membrane - Solution Interfaces by Frequency Variation and d. c. Bias Application. *J. Membr. Sci.* **1991**, *64*, 163−172.
(24) Zhao, K. S.; Hanai, T. D.c. Bias Effect on the Dielectric Behavior of Some Disperse Systems. *Bull. Inst. Chem. Res., Kyoto Univ.* **1991**, *69*, 358−374.
(25) Hanai, T.; Zhao, K. S.; Asaka, K.; Asami, K. Dielectric Theory of Concentration Polarization. Relaxation of Capacitance and Conductance for Electrolyte Solutions with Locally Varying Conductivity. *J. Membr. Sci.* **1991**, *64*, 153−161.
(26) Hanai, T.; Zhao, K. S.; Asaka, K.; Asami, K. Theoretical Approach and the Practice to the Evaluation of Structural Parameters Characterizing Concentration Polarization Alongside Ion-Exchange Membranes by Means of Dielectric Measurement. *Colloid Polym. Sci.* **1993**, *271*, 766−773.
(27) Li, Y. H.; Zhao, K. S. Dielectric Model of Concentration Polarization - Numerical Simulation for the Composite Membrane and Solution System. *Acta Chim. Sin.* **2007**, *65*, 2124−2132.
(28) Kiyohara, K.; Zhao, K. S.; Asaka, K.; Hanai, T. Determination of Capacitances and Conductances of the Constituent Phases from Dielectric Observations on Terlamellar Composite Systems. *Jpn. J. Appl. Phys.* **1990**, *29*, 1751−1756.
(29) Zhao, K. S.; Asaka, K.; Asami, K.; Hanai, T. Theory and Observation of Dielectric Relaxations due to the Interfacial Polarization for Terlamellar Structure. *Bull. Inst. Chem. Res., Kyoto Univ.* **1989**, *67*, 225−255.
(30) Nakamura, T.; Shimizu, M.; Kimura, H.; Sato, R. Effective Permittivity of Amorphous Mixed Materials. *Electron. Comm. JPN 1* **2005**, *88*, 1−9.
(31) Gouy, G. Sur la Constitution de la Charge Electrique a la Surface d'un Electrolyte. *CR Acad. Sci.* **1909**, *149*, 654−657.
(32) Gouy, G. Sur la Constitution de la Charge Electrique a la Surface d'un Electrolute. *J. Phys. (Paris)* **1910**, *9*, 457−468.
(33) Chapman, D. L. A contribution to the theory of electrocapillarity. *Philos. Mag.* **1913**, *25*, 475−481.